Physica B 403 (2008) 4156–4159

Contents lists available at ScienceDirect

Physica B

journal homepage: www.elsevier.com/locate/physb

Magnetic characterization of ferrihydrite nanoparticles synthesized by hydrolysis of Fe metal-organic precursor

E. Lima Jr.[a], A.D. Arelaro [a], H.R. Rechenberg [a], E.L. Duarte [a], R. Itri [a], C. Cavelius [b], H. Shen [b], S. Mathur [b], G.F. Goya [c,*]

[a] Instituto de Física, Universidade de São Paulo, CP 66318, 05315-970 São Paulo, Brazil
[b] Leibnitz Institute of New Materials, CVD Division, D-66123 Saarbrücken, Germany
[c] Nanoscience Institute of Aragón, University of Zaragoza, Biomedical Applications, Interfacltades II, Calle Pedro Cerbuna 12, Zaragoza 50009, Spain

ARTICLE INFO

Article history:
Received 25 July 2008
Received in revised form
21 August 2008
Accepted 27 August 2008

PACS:
75.50.Tt
76.80.+y
75.50.Dd
75.30.Gw

Keywords:
Magnetic nanoparticles
Mossbauer spectroscopy
Ferrihydrite

ABSTRACT

We investigate the formation of ferrihydrite nanoparticles (NPs) by hydrolysis of the Fe(III) alkoxide $Fe(O^tBu)_3$. Controlled amounts of water, up to 3.0 vol%, were added to the precursor solution yielding a series of hydrolyzed samples ranging from P0.0 (the unreacted precursor) to P3.0. X-ray diffraction (XRD) analysis evidenced the formation of high-crystalline ferrihydrite NP in sample P3.0, with grain size estimate of about 3.2 nm. The transition from the molecular precursor to the formation of crystalline magnetic NPs was followed through magnetization measurements $M(T)$ and $M(H)$, as well as Mössbauer spectroscopy (MS). $M(T)$ measurements indicate a paramagnetic (PM) behavior for sample P0.0, characteristic of binuclear Fe–O–Fe units, which evolves to a superparamagnetic (SPM) behavior, with an energy barrier for the blocking process estimated for sample P3.0 as $E_a = 4.9 \times 10^{-21}$ J ($E_a/k_B = 355$ K), resulting in a high effective anisotropy constant $K_{eff} = 290$ kJ/m^3. Magnetization loops at 5 K progressively change from PM-like to ferromagnetic-like shape upon increasing the hydrolysis process, although hysteresis ($H_c \approx 500$ Oe) only is apparent for P2.0 and higher. MS spectra at room temperature are PM/SPM doublets for all samples, while the MS spectra at $T = 4.2$ K reveal increasingly well-defined magnetic ordering as hydrolysis of the precursor stepwise progresses until well-crystallized ferrihydrite particles are formed.

1. Introduction

Magnetic nanoparticles (NPs) have been the subject of growing interest from both fundamental [1] and technological [2] points of view, because, within a few-nanometer scale, their magnetic properties strongly differ from those of bulk material. Specially, iron oxide NPs are of great interest owing to their potential application in biomedicine [3], where requirements of low toxicity levels as well as a large saturation magnetic moment are crucial.

Iron oxides and oxyhydroxides are globally of great importance in the environment as well as in industry. In this family, ferrihydrite, which occurs naturally in the 3–5 nm particle size range [4,5], is an Fe(III) oxyhydroxide of considerable importance in mineralogy and metallurgical processing. It is a naturally occurring hydrated ferric oxyhydroxide mineral and can also be synthesized easily (e.g., by rapid oxidation of Fe^{2+}-containing solutions followed by hydrolysis [4–6]) and it is a precursor to other iron oxides such as hematite [7]. A number of formulas have been proposed for ferrihydrite structure (e.g., $5Fe_2O_3 \cdot 9H_2O$, $Fe_5HO_8 \cdot 4H_2O$) but they are all equivalent to $FeOOH \cdot nH_2O$ [8]. In fact, detailed crystal structure of this poorly crystalline Fe^{3+} oxyhydroxide has remained elusive up to now, as reflected by the identification of the known phases as 'two-line' and 'six-line' on the basis of their two or six broad X-ray diffraction (XRD) peaks.

Magnetic properties of ferrihydrite are also controversial. In general, ferrimagnetic and antiferromagnetic states are attributed to the two-line and six-line species, respectively [9]. Neutron diffraction analysis reveals that six-line ferrihydrite has an ordered antiferromagnetic state with Néel temperature extrapolated to about 330 K [4]. However, ferrihydrite NPs have a magnetic moment/particle $\mu_p = 300\mu_B$, which could be explained by a random distribution of uncompensated spins of Fe [6].

NPs of iron oxyhydroxide were synthesized with several chemical routes [10] because this approach to produce samples allows synthesizing nanocrystalline material from smaller molecular units. Therefore, a nanocrystalline material with new properties can be designed and produced from a well-defined

* Corresponding author. Tel.: +34 976 76 27 83; fax: +34 976 76 27 76.
E-mail address: goya@unizar.es (G.F. Goya).

0921-4526/$ - see front matter © 2008 Elsevier B.V. All rights reserved.
doi:10.1016/j.physb.2008.08.018

'building unit'. In this way, chemical processing of metal-organic precursor molecules is a powerful route for the synthesis of nanocrystalline materials with controlled homogeneity and narrow particle size distribution [11].

For the present investigation, the single-source approach [12] was used, which allows synthesizing nanocrystalline material from smaller molecular units acting as well-defined building units. In this way, chemical processing of metal-organic precursor molecules constitutes a powerful route for the syntheses of nanocrystalline materials with controlled homogeneity and narrow particle size distribution. Finally, magnetic properties and Mössbauer data were used to monitor the formation of iron oxyhydroxide NPs by hydrolysis of a Fe(III) precursor compound, controlling the hydrolysis process to produce samples with different crystallinity and grain size.

2. Experimental

2.1. Synthesis procedure

Fe(III) alkoxide $Fe(O^tBu)_3$ was partially hydrolyzed by reacting with stoichiometric amounts of water to obtain poly-nuclear iron containing oxo-hydroxo clusters. For this purpose, we started from 0.9 m mol of pure and unhydrolyzed iron alkoxide, which was dissolved in 2 ml freshly distilled styrene monomer and thermally polymerized at 80 °C for 30 min by addition of 15 mg dry Dibenzoylperoxide (DBPO) as polymerization starter. The samples were labeled as P*x*, where *x* indicates the H_2O:Fe molar ratio used. In all, four samples were prepared: P0.0, P0.8, P2.0 and P3.0 where the expected hydrolysis degrees were 0%, 26%, 66% and 100%, respectively. After polymerization, the polystyrene–polymer was cut into discs for Mössbauer and SQUID measurements.

2.2. Apparatus

The transition from the molecular precursor until the formation of crystalline magnetic NPs was followed through magnetization measurements as well as Mössbauer spectroscopy (MS). XRD patterns were obtained in a Philips PW–1140 diffractometer using Cu–K_α radiation ($\lambda_{\alpha 1} = 1.54060$ Å). Static and dynamic magnetic measurements as a function of frequency and temperature were performed in a commercial SQUID MPMS-xl magnetometer (quantum design). Zero-field-cooled (ZFC) and field-cooled (FC) curves were taken between 5 and 300 K, with cooling field $H_{FC} = 100$ Oe. Data were obtained by first cooling the sample from room temperature (RT) in zero applied field (ZFC process) to the basal temperature (5 K). Then a field was applied and the variation of magnetization was measured with increasing temperature up to $T = 300$ K. After the last point was measured, the sample was cooled again to the basal temperature keeping the same field (FC process); then the M vs. T data were measured for increasing temperatures. The frequency dependences of both in-phase $\chi'(T)$ and out-of-phase $\chi''(T)$ components of the ac magnetic susceptibility were measured by using an excitation field of 1–4 Oe and driving frequencies 0.01 Hz $< f <$ 1500 Hz. MS measurements were performed with a conventional constant acceleration spectrometer in transmission geometry with a source of about 50 mCi ^{57}Co in an Rh matrix between 4.2 and 296 K. Hyperfine parameters such as the distribution of hyperfine magnetic field, isomer shift and quadrupole shift have been determined by NORMOS program and α-Fe at 296 K was used to calibrate isomer shifts and velocity scale.

3. Results

Fig. 1 presents ZFC and FC curves of all samples measured in $H = 50$ Oe. $M(T)$ data on sample P0.0 show the expected paramagnetic (PM) behavior for the unreacted precursor compound, although the $M^{-1}(T)$ curve at low temperature (inset of Fig. 1) deviates from a simple Curie law. This may be associated to Fe–Fe exchange coupling within the core of the precursor units. Magnetization curves $M(T)$ of sample P0.8 exhibits a predominant PM characteristic with two distinct linear slopes, above and below 170 K. This is possibly related to the mixture of the magnetic behaviors of the molecular precursor and incipiently crystallized material, both present in this sample. It should be noted that

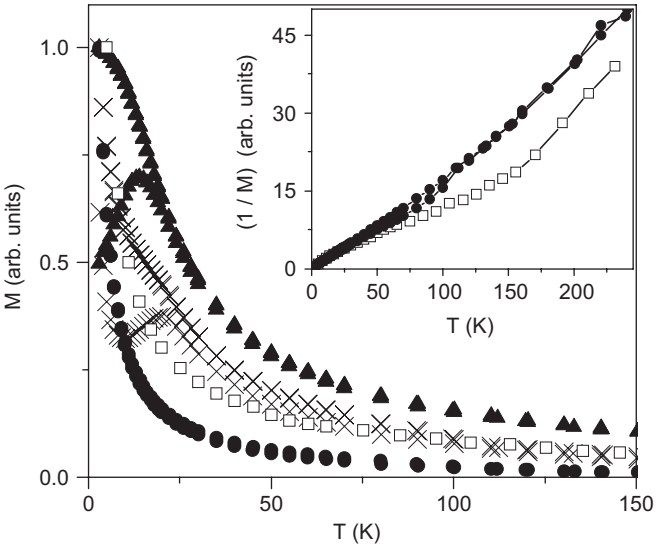

Fig. 1. $M(T)$ (in ZFC and FC modes) measured with $H = 50$ Oe of samples P0.0 (solid circles), P0.8 (open squares), P2.0 (crosses) and P3.0 (solid triangles). Inset presents the M^{-1} vs. T curves of samples P0.0 and P0.8.

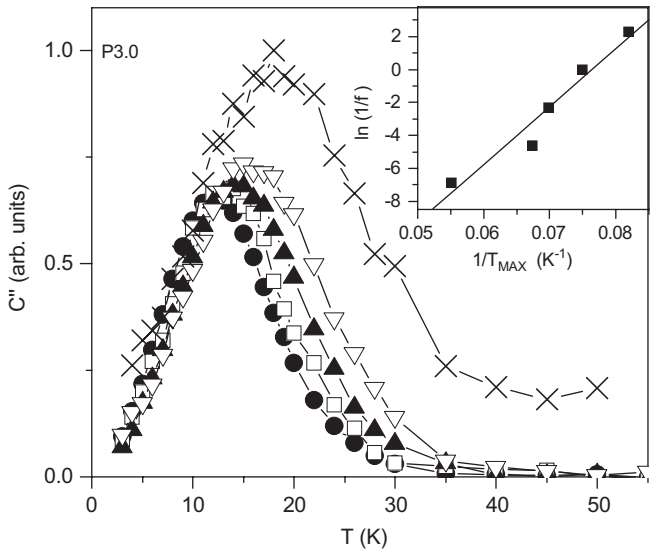

Fig. 2. Plot of imaginary component of ac susceptibility χ'' vs. temperature for sample P3.0 measured at different frequency values: 0.1 Hz (solid circles), 1 Hz (open squares), 10 Hz (solid up triangles), 100 Hz (open down triangles) and 1000 Hz (crosses). Inset: plot of $\ln(1/f)$ vs. $1/T_{max}$ obtained from the ac measurement. Solid line represents the linear fit with Eq. (1).

absolute magnetization values could not be obtained due to the presence of the polystyrene matrix (Fig. 2).

Sample P2.0 exhibits a mixed PM–superparamagnetic (SPM) behavior, with a peak in the ZFC curve at T_{max} due to blocking process of crystalline units within this sample, which presents internal magnetic order. The low value of $T_{max}\sim 20$ K indicates a small crystalline size since $T_B = T_{max} \cong 25\, K_{eff} V/k_B$ for dc magnetization measurements, where V is the particles volume and K_{eff} is the effective anisotropy constant.

$M(T)$ measurements on sample P3.0 clearly reveal a SPM behavior, with a peak in the ZFC curve at $T_{max} = 14$ K. ZFC and FC curves split for $T_{irr} = 28$ K, not so close to T_{max}, indicating a comparatively broad distribution of the blocking temperature, since T_{irr} indicates the highest blocking temperature. There is no evidence of a PM regime, showing the complete transition from the molecular precursor to the magnetic regime dominated by ferrihydrite NPs with internal magnetic order.

The $M(H)$ curves measured at 5 K (below T_{max} of samples P2.0 and P3.0) in fields up to 70 kOe change progressively from a PM pattern for samples P0.0 to a typical ferromagnetic shape for sample P3.0. Fig. 3 displays the low-field region of the $M(H)$ curves of all samples. For samples P0.0 and P0.8, no hysteresis is observed, while samples P2.0 and P3.0 exhibit a coercive field $H_C = 500$ Oe. The $M(H)$ curve of sample P3.0 exhibits saturation for fields higher than about 20 kOe (see inset of Fig. 3). The absence of saturation in the $M(H)$ curves of the other samples is related to the presence of the PM component.

XRD profile of sample P3.0 (Fig. 4) shows a very broad peak at low angles (full dots) originated in the polymeric matrix, and a set of narrower peaks at higher angles (open squares) originated in a crystalline phase. The latter contribution could be indexed using the six-line ferrihydrite phase [13]. Substraction of the organic background allowed to apply Scherrer's formula to the most intense peaks of ferrihydrite phase, obtaining an average particle diameter $d = 3.2$ nm for sample P3.0.

Further characterization was performed by MS. At RT natural and synthetic samples are SPM and their spectra show asymmetrically broadened quadrupole splitting originated in structural distortion of the average Fe^{3+} site [6]. For the present samples, all Mössbauer spectra taken at RT (not shown) display a central (PM) doublet with quadrupolar splitting QS = 0.72 mm/s and isomer shift IS = 0.36 mm/s. However, the MS spectra collected at 4.2 K show different characteristics. For sample P0.0 (Fig. 5(a)), the spectrum consists of a doublet plus a sextet with broad lines and hyperfine field $B_{hf} = 42.5$ T, which could indicate incipient crystallization of the ferrihydrite phase. However, the spectrum as a whole might as well arise from slow relaxation of PM Fe^{3+} ions [6]. For increasingly hydrolyzed samples, the magnetic order is observed to increase, with the presence of two sextets with mean $B_{hf} = 47.8$ T, in agreement with literature data for ferrihydrite NPs [14]. The relative area of the magnetic sextet grows with increase in hydrolysis process, being the only contribution in the MS spectrum of sample P3.0 at 4.2 K (Fig. 5(b)). Therefore, our MS data confirm the evolution of the system from the precursor molecular structure towards ferrihydrite NPs on increasing the

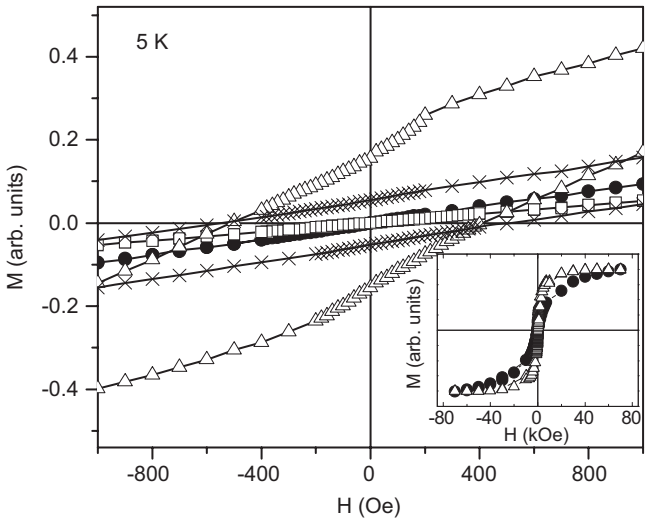

Fig. 3. Low-field region of $M(H)$ curves of samples P0.0 (solid circles), P0.8 (opens squares), P2.0 (crosses) and P3.0 (open triangles) measured at 5 K and field up to 70 kOe. Inset shows the complete magnetization curves of samples P0.0 and P0.3.

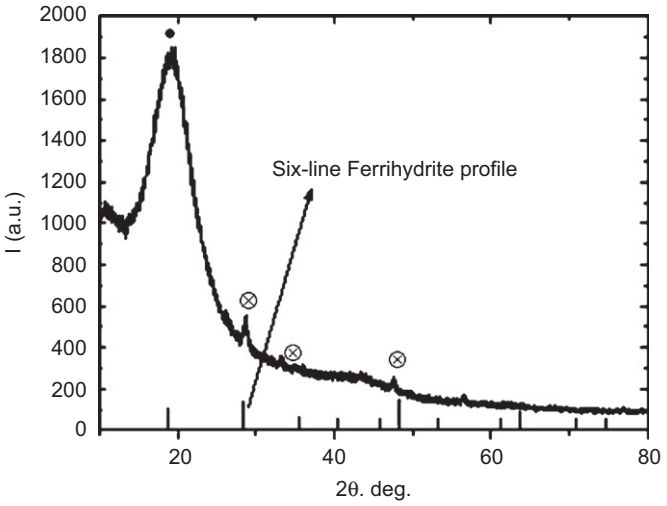

Fig. 4. X-ray diffraction profile of sample P3.0. Full dots denote the polymeric matrix contribution while crossed circles indicate the most intense peaks of the six-line ferrihydrite phase. A crystallite size of $d = 3.2$ nm was obtained from Scherrer's formula.

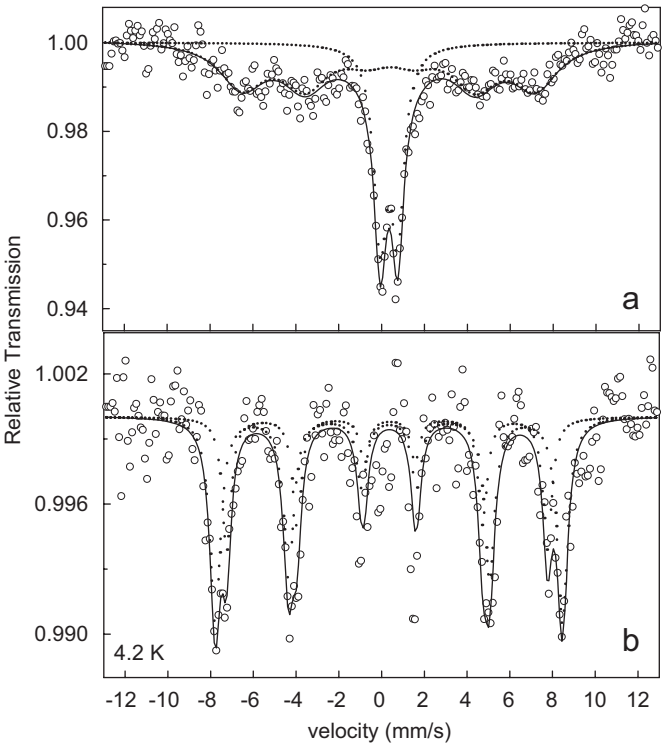

Fig. 5. Mössbauer spectra collected at 4.2 K of samples: (a) P0.0 and (b) P3.0. Solid lines are the fitted experimental spectra and dashed lines correspond to each component of the spectrum.

hydrolysis process, as observed from the magnetic properties of the four samples.

4. Discussion

The $Fe(O^tBu)_3$ unit used as precursor has three alkoxide–iron bonds which could be hydrolyzed. P3.0 means that three parts of water were added referred to the molar amount of precursor in solution. This means that for this case all possible bonds were hydrolyzed. P2.0 means that 66% percent or two bonds of a precursor molecule were hydrolyzed. Finally, P0.8 means that only 26% of all precursor bonds in the solution were finally hydrolyzed.

Theoretically, a molar H_2O:Fe ratio of 1.5 is sufficient for complete hydrolysis and condensation, since water is produced as a by-product of the condensation reaction. However, previous investigations suggest that only partial hydrolysis may occur, since several intermediate species can be formed, with formulas $[FeO_x(OH)_y(OR)_z]$; $2x+y+z=3$. Therefore, it is expected that a shift from PM to the SPM behavior of the particles could only be observed by application of an excess of water (i.e., samples P2.0 and P3.0). The present $M(T)$ curves showing a blocking process only for P3.0 sample support this mechanism.

After hydrolysis, a condensation process in which the polymeric network is formed takes place (in our case, the condensation process is stopped by finishing the polymerization after 30 min and subsequent curing of the polymer). Formation of ferrihydrite phase is possible only if all bonds are hydrolyzed, and hence only for sample P3.0 the crystallized phase could be observed. The T_B value observed for sample P2.0 is slightly higher when compared to that of sample P3.0, and this could be related to clustering of the incipient particles due to a shorter polymerization time of the polystyrene matrix for P2.0 sample.

Regarding the evolution of the magnetic properties with increase in hydrolysis time, the results for P3.0 indicate a SPM behavior with a T_B value (as obtained from ZFC data) similar to the previously reported for ferrihydrite NPs. Regarding the variation of T_{max} with measuring frequency for sample P3.0, the results from the imaginary component of the ac susceptibility $\chi''(f,T)$ (Fig. 2) confirm the thermal activation blocking process. We estimate the activation energy through a linear fit of $\ln(1/f)$ vs. $1/T_{max}$ (see inset of Fig. 2) according to the following equation:

$$f = f_0 \exp(-E_a/k_B T) \quad (1)$$

where f_0 is a characteristic frequency. The values obtained from the fit were $E_a = 4.9\times10^{-21}$ J ($E_a/k_B = 355$ K) and $f_0^{-1} = \tau_0 = 1.9\times10^{-12}$ s. Using $d = 3.2$ nm obtained from XRD analysis and $E_a = 4.9\times10^{-21}$ J, one obtains $K_{eff} = 290$ kJ/m^3, close to the value expected for ferrihydrite NPs [15].

In summary, we have studied the formation of ferrihydrite NPs from molecular iron clusters $Fe(O^tBu)_3$ by water hydrolysis. The gradual transition from PM to SPM behavior was observed through the appearance of long-range magnetic order. Magnetization loops at 5 K progressively change from PM-like to ferromagnetic-like shape for increasing hydrolysis time, confirming the long-range order. For the final ferrihydrite NPs, the anisotropy energy barrier was found to be $E_a = 4.9\times10^{-21}$ J. Mössbauer spectra at $T = 4.2$ K reveal increasingly well-defined magnetic ordering, as hydrolysis of the precursor stepwise progresses until ferrihydrite particles are formed.

Acknowledgements

This work was financially supported by VW Foundation, FAPESP and CNPq agencies. G.F.G. acknowledges support from the Spanish MEC through the Ramon y Cajal program.

References

[1] E.M. Chudnovsky, J. Tejada, Macroscopic Quantum Tunneling of the Magnetic Moment, Cambridge University Press, Cambridge, UK, 1994.
[2] R.W. Chantrell, K. O'Grady, in: R. Gerber, C.D. Wright, G. Asti (Eds.), Applied Magnetism, Kluwer Academic Publishers, The Netherlands, 1994, p. 113.
[3] I. Hilger, A. Kiessling, E. Tomanus, R. Hiergeist, R. Hergt, W. Andrä, M. Roskos, W. Linss, P. Weber, W.A. Kaiser, Nanotechnology 15 (2004) 1027.
[4] E. Jansen, A. Kyek, W. Schäfer, U. Schwertmann, Appl. Phys. A 74 (2002) S1004.
[5] N.J.O. Silva, V.S. Amaral, L.D. Carlos, B. Rodriguez-Gonzalez, L.M. Liz-Marzan, T.S. Berquo, S.K. Banerjee, V.D. Bermudez, A. Millan, F. Palacio, Phys. Rev. B 77 (2008) 134426.
[6] A. Punnoose, T. Phanthavady, M.S. Seehra, N. Shah, G.P. Huffman, Phys. Rev. B 69 (2204) 054425.
[7] Udo Schwertmann, Josef Friedl, Helge Stanjek, J. Colloid Interface Sci. 209 (1999) 215.
[8] F.E. Huggins, Z. Feng, F. Lu, N. Shah, G.P. Huffman, J. Catal. 143 (1993) 499.
[9] Q.A. Pankhurst, R.J. Pollard, Clays Clay Miner. 40 (1992) 268.
[10] E. Murad, U. Schwertmann, Am. Mineral. 65 (1980) 1044.
[11] J.P. Jolivet, C. Chanéac, E. Tronc, Chem. Commun. 5 (2004) 477.
[12] H. Shen, S. Mathur, J. Physique IV 12 (2002) (Pr4-1, and references cited therein).
[13] U. Schwertmann, F. Wagner, H. Knicker, Soil Sci. Soc. Am. J. 69 (2005) 1009.
[14] I.P. Suzdalev, V.N. Buravtsev, V.K. Imshennik, Yu.V. Maksimov, V.V. Matveev, S.V. Novichikhin, A.X. Trautwein, H. Winkler, Z. Phys. D 37 (1996) 55.
[15] E.L. Duarte, R. Itri, E. Lima Jr., M.S. Baptista, T.S. Berquo, G.F. Goya, Nanotechnology 17 (2006) 5549.